Constr. Approx. (1993) 9: 209–236

CONSTRUCTIVE APPROXIMATION

Compactly Supported Bidimensional Wavelet Bases with Hexagonal Symmetry

A. Cohen and J.-M. Schlenker

Abstract. We study a class of subband coding schemes allowing perfect reconstruction for a bidimensional signal sampled on the hexagonal grid. From these schemes we construct biorthogonal wavelet bases of $L^2(\mathbf{R}^2)$ which are compactly supported and such that the sets of generating functions ψ_1, ψ_2, ψ_3 for the synthesis and $\tilde{\psi}_1, \tilde{\psi}_2, \tilde{\psi}_3$ for the analysis, as well as the scaling functions φ and $\tilde{\varphi}$, are globally invariant by a rotation of $2\pi/3$. We focus on the particular case of linear splines and we discuss how to obtain a higher regularity. We finally present the possibilities of sharp angular frequency resolution provided by these new bases.

1. Introduction

1.1. Wavelet Bases of $L^2(\mathbf{R})$

Wavelet bases are families of functions of the type

$$\psi_k^j(x) = 2^{-j/2}\psi(2^{-j}x - k), \tag{1}$$

where ψ is a mother function in $L^2(\mathbf{R})$ well localized both in time and frequency. They are usually defined with the help of a multiscale analysis, i.e., a sequence of approximation subspaces $\{V_j\}_{j\in\mathbf{Z}}$ of $L^2(\mathbf{R})$ associated with a scaling function $\varphi(x)$ such that

$$\{0\} \cdots \to V_2 \subset V_1 \subset V_0 \subset V_{-1} \subset V_{-2} \cdots \to L^2(\mathbf{R}), \tag{2}$$

$$f(x) \in V_j \Leftrightarrow f(2x) \in V_{j-1} \Leftrightarrow f(2^j x) \in V_0, \tag{3}$$

$$\{\varphi(x-k)\}_{k\in\mathbf{Z}} \text{ is an orthonormal basis for } V_0. \tag{4}$$

In this framework, wavelets characterize, at each scale, the necessary details to get from one level of approximation to the next finer level since $\{\psi_k^j\}_{k\in\mathbf{Z}}$ forms a hilbertian basis for the orthogonal complement W_j of V_j into V_{j-1} (see [Me], [D1], and [D2]).

Date received: October 4, 1991. Date revised: September 28, 1992. Communicated by Charles A. Micchelli.

AMS classification: Primary 41A63, 46C99; Secondary 41A30, 41A15, 42B99, 46E20.

Key words and phrases: Courant interpolating function, Linear splines, Hexagonal filter banks, Biorthogonal wavelets, Multiresolution analysis.

In practice (see [D1]) the starting point to multiresolution analysis and wavelets is a pair of digital filters represented by their transfer functions $m_0(\omega)$ and $m_1(\omega) = e^{-i\omega}m_0(\omega + \pi)$ that satisfy

$$m_0(0) = 1 \tag{5}$$

and

$$|m_0(\omega)|^2 + |m_0(\omega + \pi)|^2 = 1. \tag{6}$$

The scaling function and the wavelet are then defined by

$$\hat{\varphi}(\omega) = \prod_{k=1}^{+\infty} m_0(2^{-k}\omega) \quad \text{and} \quad \hat{\psi}(\omega) = m_1\left(\frac{\omega}{2}\right)\hat{\varphi}\left(\frac{\omega}{2}\right). \tag{7}$$

These filters, called "conjugate quadrature filters," are also used in the Fast Wavelet Transform Algorithm: A discrete signal is split into two sequences of approximation and detail coefficients at the next coarser scale, by convolution with the low-pass filter m_0 and the high-pass filter m_1, followed by the decimation of one sample out of two (the total amount of information is preserved). The reconstruction is operated by the same filters that are used to interpolate and refine the decimated sequences, followed by a normalization of a factor 2. This set of operations is known in electrical engineering as a Subband Coding Scheme.

A multiscale representation of the original signal is obtained by iterating the decomposition on the coarse approximation, but the details can also be decomposed for more frequency resolution: this generalization leads to the "wavelet-packets analysis" [CMQW] that we use in Section 5 of this paper.

The class of compactly supported wavelets [D1] is particularly interesting for the applications since the conjugate quadrature filters corresponding to such bases have finite impulse responses and the subband coding scheme which constitutes each step of the algorithm can thus be implemented very easily.

1.2. Biorthogonal Wavelet Bases

Biorthogonal wavelets were designed to obtain wider possibilities in the choice of the functions used in a wavelet basis.

In this more general setting, introduced in [CDF], one starts from a two-channel subband coding scheme with perfect reconstruction, where the analysis and synthesis filters need not be identical as in the particular case of the CQF.

In one dimension this leads to a pair of dual low-pass filters represented by their transfer functions $\tilde{m}_0(\omega)$ (for the analysis) and $m_0(\omega)$ (or the synthesis) which have to satisfy the following relations:

$$m_0(0) = \tilde{m}_0(0) = 1 \quad \text{and} \quad m_0(\pi) = \tilde{m}_0(\pi) = 0, \tag{8}$$

$$\overline{m_0(\omega)}\tilde{m}_0(\omega) + \overline{m_0(\omega + \pi)}\tilde{m}_0(\omega + \pi) = 1. \tag{9}$$

If m_0 is fixed, finding $\tilde{m}_0$ can be done by solving a Bezout problem or inverting a finite matrix. The two high-pass filters that are used to compute detail information are simply expressed by

$$m_1(\omega) = e^{-i\omega}\overline{\tilde{m}_0(\omega + \pi)} \quad \text{and} \quad \tilde{m}_1(\omega) = e^{-i\omega}\overline{m_0(\omega + \pi)}. \tag{10}$$

The associated scaling functions and wavelets are defined in the same way as for the orthonormal case but the synthesis functions $\{\varphi, \psi\}$ and the analyzing functions $\{\tilde{\varphi}, \tilde{\psi}\}$ need not be identical. We have

$$\hat{\varphi}(\omega) = \prod_{k=1}^{+\infty} m_0(2^{-k}\omega) \quad \text{and} \quad \hat{\psi}(\omega) = m_1\left(\frac{\omega}{2}\right)\hat{\varphi}\left(\frac{\omega}{2}\right), \tag{11}$$

$$\hat{\tilde{\varphi}}(\omega) = \prod_{k=1}^{+\infty} \tilde{m}_0(2^{-k}\omega) \quad \text{and} \quad \hat{\tilde{\psi}}(\omega) = \tilde{m}_1\left(\frac{\omega}{2}\right)\hat{\tilde{\varphi}}\left(\frac{\omega}{2}\right). \tag{12}$$

Clearly, $m_0 = \tilde{m}_0$ gives the orthonormal-CQF case. Then, under additional conditions detailed in [CDF], [C], and [CD1] and briefly recalled in the appendix, we have, for any f in $L^2(\mathbf{R})$,

$$f = \sum_{j,k \in \mathbf{Z}} \langle f | \tilde{\psi}_k^j \rangle \psi_k^j, \tag{13}$$

where these expansions are unique and unconditional (i.e., stable in the L^2 sense).

1.3. Tensorial Wavelet Bases of $L^2(\mathbf{R}^2)$

The usual method to generalize wavelet bases the multiscale analysis to n-dimensional functions is based on tensor products. This method is valid for biorthogonal as well as for orthonormal wavelets. For example, in two dimensions, the space V_j are generated by the families $\{2^{-j}\varphi(2^{-j}x - k)\varphi(2^{-j}y - \ell)\}_{(k,\ell)\in\mathbf{Z}^2}$ and three wavelets are necessary to characterize the details: $\psi(x)\varphi(y)$, $\varphi(x)\psi(y)$, and $\psi(x)\psi(y)$ which represent in image processing respectively the horizontal, vertical and "corner" edges (see [Ma]). This allows the use of all the results established in the unidimensional case about the regularity and oscillation properties of compactly supported wavelets. However, the tensor product construction is clearly restrictive and, moreover, it leads to a nonisotropic analysis for two reasons:

(a) The horizontal and vertical directions have a particular importance and the three wavelets are not "equivalent," in the sense that only the first two can be exchanged by a transformation on the coordinates $((x, y) \to (y, x))$.
(b) It is known that compactly supported scaling functions and wavelets in one dimension cannot be symmetrical (except for the Haar system which is composed of discontinuous functions, see [D1]), and that can be a problem for some applications such as image coding.

1.4. The Hexagonal Lattice

The hexagonal lattice Γ in $\mathbf{R}^2$ can be defined as the image of $\mathbf{Z}^2$ by a linear transformation corresponding to the matrix $\begin{pmatrix} 1 & -\frac{1}{2} \\ 0 & \sqrt{3}/2 \end{pmatrix}$.

One can also write

$$\Gamma = \{n_1 e_1 + n_2 e_2 + n_3 e_3 | (n_1, n_2, n_3) \in \mathbf{Z}^3\}, \tag{14}$$

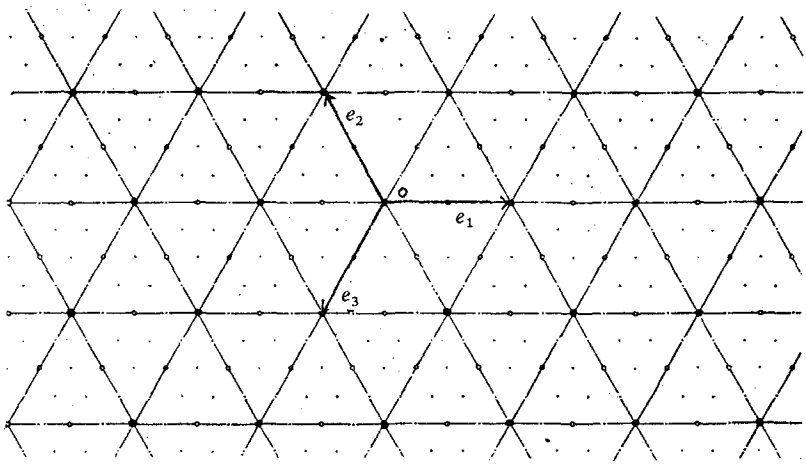

(a)

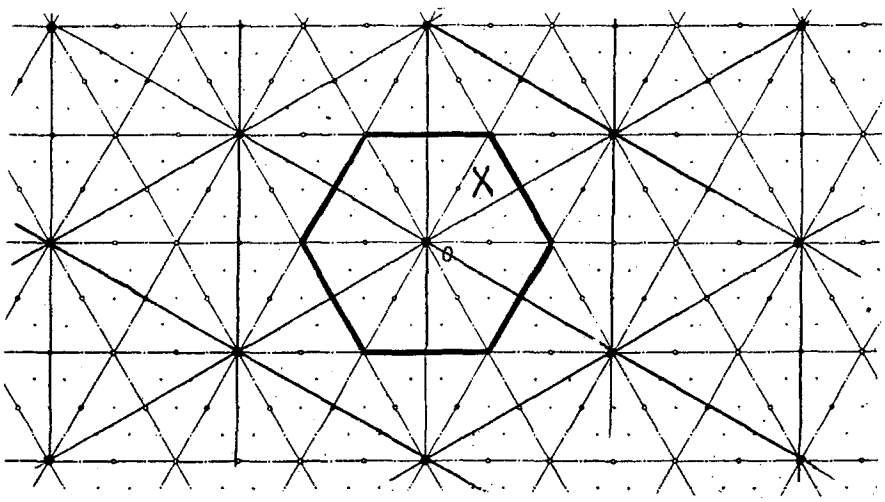

(b)

Fig. 1 (a) The hexagonal mesh Γ and (b) the dual lattice $\hat{\Gamma}$ and its Voronoic cell X.

the vectors e_1, e_2, e_3 being defined in Fig. 1(a); they are not independent, but the coordinate system $(\omega_1, \omega_2, \omega_2)$ given by

$$\omega_1 = \langle \omega | e_1 \rangle, \qquad \omega_2 = \langle \omega | e_2 \rangle, \quad \text{and} \quad \omega_3 = \langle \omega | e_3 \rangle \tag{15}$$

is useful because it reflects the symmetries of the lattice. For any point $\omega \in \mathbf{R}^2$, we have

$$\omega_1 + \omega_2 + \omega_3 = 0. \tag{16}$$

The hexagonal lattice has two related interesting properties:

- It is "compact" in the sense that it allows the densest repartition of points in $\mathbf{R}^2$ with given minimal distance between them.
- It is "isotropic" since it has three equivalent main directions (against, for instance, only two for the "square" lattice).

We define a filter on Γ as an element of $l^2(\Gamma, \mathbf{R})$. The ring of compactly supported filters is denoted by $\mathscr{CF}$, its multiplication being the usual convolution product. For each filter $\{h_\gamma\}_{\gamma\in\Gamma}$, the associated transfer function is defined on $\mathbf{R}^2$ by the discrete Fourier transform

$$m(\omega) = \sum_{\gamma\in\Gamma} h_\gamma e^{-i\langle\omega|\gamma\rangle}. \tag{17}$$

The "dual lattice" $\hat{\Gamma}$ to Γ is the set of points ω in $\mathbf{R}^2$ such that, for all $\gamma\in\Gamma$, $\langle\omega|\gamma\rangle$ is an integer multiple of 2π. It is also an hexagonal lattice that can be obtained by rotating Γ of $\pi/6$ and dilating the result by $4\pi/\sqrt{3}$. The "Voronoi cell" X of the dual lattice—that is, the set of points closer to 0 than to any other point of the dual lattice—is thus the minimal domain of $\mathbf{R}^2$ on which the transfer function of a filter has to be known. In the one-dimensional case this domain is the interval $[-\pi, \pi]$. In the two-dimensional hexagonal case it is an hexagon.

Some graphs related to Γ are shown in Fig. 1.

1.5. Hexagonal Wavelets

This paper deals with the two problems of tensorial bidimensional wavelets mentioned above and presents an original construction which allow more isotropy. We use the hexagonal mesh Γ instead of $\mathbf{Z}^2$ as the translation group associated with V_0. We still need *a priori* three wavelets to characterize the details, but we shall see that it is possible to choose a scaling function φ invariant by a rotation of $2\pi/3$ and the three wavelets ψ_1, ψ_2, and ψ_3 such that $\{\psi_1, \psi_2, \psi_3\}$ is globally invariant by a rotation of $2\pi/3$. That is, we have only one wavelet, but we are adding a $2\pi/3$ rotation to the set of transformations generating the elements of the basis from this wavelet.

In the biorthogonal setting, this leads to

Definition 1.5.1. A hexagonal biorthogonal wavelet basis of $L^2(\mathbf{R}^2)$ is a biorthogonal wavelet basis such that the sets $\{\psi_1, \psi_2, \psi_3\}$ and $\{\tilde{\psi}_1, \tilde{\psi}_2, \tilde{\psi}_3\}$, as well as the scaling functions φ and $\tilde{\varphi}$, are globally invariant by a $2\pi/3$ rotation.

This idea, due to Y. Meyer and S. Jaffard, was introduced to construct a wavelet basis of $L^2(\mathbf{R}^2)$ where all the generating functions are piecewise affine on the triangles of $\frac{1}{2}\Gamma$ (see [Me] and [J]). In this case V_0 is the space of square integrable piecewise affine functions on the triangles of Γ. A natural generator for V_0 is given by the Courant interpolating "hat function" φ represented in Fig. 3(a). However, the family $\{\varphi(x-\gamma)\}_{\gamma\in\Gamma}$ is clearly nonorthonormal. Using the gramian matrix

$G = (\langle \varphi(x-\gamma) | \varphi(x-\gamma') \rangle)_{(\gamma,\gamma') \in \Gamma^2}$, an orthonormal basis can be generated by

$$(\varphi_0(x-\gamma))_{\gamma\in\Gamma} = G^{-1/2}(\varphi(x-\gamma))_{\gamma\in\Gamma}.$$

The new scaling function φ_0 has hexagonal symmetry like φ, orthonormal translates by Γ, but no compact support.

More generally, it seems difficult to build orthonormal bases of compactly supported bidimensional wavelets without the help of the tensor product method. It is necessary to design the nonseparable finite impulse response CQF and the Fejer–Riesz lemma which is crucial in one dimension to derive the transfer function from its square modulus (see [D1]) but does not generalize in the multidimensional framework. For this reason we leave the orthonormality constraint and consider biorthogonal bases of wavelets.

Another interesting construction, made by C. K. Chui, J. Stöckler, and J. Ward, leads to compactly supported spline wavelets, but the dual functions (and the analysing filters) are not compactly supported (see [CSW]). Finally, an article by C. de Boor, K. Höllig, and S. Riemenschneider deals with the use of various box splines for bivariate cardinal interpolation but their approach and their results are quite different from ours (see [BHR]): a mapping is used to derive the high-pass filters from the low-pass via

$$\begin{cases} m_1(\omega_1,\omega_2,\omega_3) = e^{i\omega_1} m(\omega_1+\pi, \omega_2+\pi, \omega_3), \\ m_2(\omega_1,\omega_2,\omega_3) = e^{i\omega_2} m(\omega_1, w_2+\pi, \omega_3+\pi), \\ m_3(\omega_1,\omega_2,\omega_3) = e^{i\omega_3} m(\omega_1+\pi, \omega_2, \omega_3+\pi). \end{cases} \tag{18}$$

We have used here the representation $\omega = (\omega_1, \omega_2, \omega_3)$ that is defined in (1.4). This is also the mapping that was used by Y. Meyer and S. Jaffard in the orthonormal case. In our approach we are particularly concerned to have finite impulse response filters for both the decomposition and the reconstruction of our two-dimensional signals. We shall see that, with this requirement, the high-pass filters cannot be derived from the previous mapping.

We, of course, have a similar definition for the filters:

Definition 1.5.2. A family $\{m_0, \ldots, m_3, \tilde{m}_0, \ldots, \tilde{m}_3\}$ of filters has hexagonal symmetry if the sets $\{m_1, \ldots, m_3\}$ and $\{\tilde{m}_1, \ldots, \tilde{m}_3\}$, as well as the filters m_0 and $\tilde{m}_0$, are globally invariant by a $2\pi/3$ rotation.

This can be expressed by the following identities:

$$\begin{cases} m(\omega_1,\omega_2,\omega_3) = m(\omega_2,\omega_3,\omega_1) = m(\omega_3,\omega_1,\omega_2), \\ m_1(\omega_1,\omega_2,\omega_3) = m_2(\omega_3,\omega_1,\omega_2) = m_3(\omega_2,\omega_3,\omega_1) \end{cases} \tag{19}$$

(also valid for $\{\tilde{m}_0, \ldots, \tilde{m}_3\}$). After imposing some specific conditions, described in the next section, on these filters, we define our scaling functions and wavelets in a similar way to the one-dimensional case by

$$\hat{\psi}(\omega) = \prod_{k=1}^{+\infty} m_0(2^{-k}\omega) \quad \text{and} \quad \hat{\tilde{\varphi}}(\omega) = \prod_{k=1}^{+\infty} \tilde{m}_0(2^{-k}\omega), \tag{20}$$

$$\hat{\psi}_\varepsilon(2\omega) = m_\varepsilon(\omega)\hat{\varphi}(\omega) \quad \text{and} \quad \hat{\tilde{\psi}}_\varepsilon(2\omega) = \tilde{m}_\varepsilon(\omega)\hat{\tilde{\varphi}}(\omega) \qquad \text{for} \quad \varepsilon = 1, 2, 3. \tag{21}$$

A trivial result links hexagonal filters to hexagonal wavelets:

Proposition 1.5.3. *Let* $\{m_0, \ldots, m_3, \tilde{m}_0, \ldots, \tilde{m}_3\}$ *be a family of filters associated with a biorthongonal wavelet basis; then the wavelet basis is hexagonal if and only if* $\{m_0, \ldots, m_3, \tilde{m}_0, \ldots, \tilde{m}_3\}$ *is hexagonal.*

Proof. If $\{m_0, \ldots, m_3, \tilde{m}_0, \ldots, \tilde{m}_3\}$ is hexagonal, then the associated scaling functions φ and $\tilde{\varphi}$ are invariant under a $2\pi/3$ rotation by (20), since m_0 and $\tilde{m}_0$ have the same invariance. Then, by (21), $\{\psi_1, \psi_2, \psi_3\}$ and $\{\tilde{\psi}_1, \tilde{\psi}_2, \tilde{\psi}_3\}$ are globally invariant by a $2\pi/3$ rotation.

Reciprocally, the invariance by $2\pi/3$ rotation of φ and $\tilde{\varphi}$ means the invariance of m_0 and $\tilde{m}_0$ (remarking that $\hat{\varphi}(2\omega) = m_0(\omega)\hat{\varphi}(\omega)$ and $\hat{\tilde{\varphi}}(2\omega) = \tilde{m}_0(\omega)\hat{\tilde{\varphi}}(\omega)$), and then the invariance of $\{\psi_1, \psi_2, \psi_3\}$ and $\{\tilde{\psi}_1, \tilde{\psi}_2, \tilde{\psi}_3\}$ implies the invariance of $\{m_1, m_2, m_3\}$ and of $\{\tilde{m}_1, \tilde{m}_2, \tilde{m}_3\}$ by (21). ■

2. Perfect Reconstruction Hexagonal Filters

2.1. Subband Coding Scheme

We now take a closer look at the transfer functions of the digital filters that will lead us to the construction of our hexagonal biorthogonal wavelet bases. Since we want to express in a simple way the hexagonal symmetry constraints that we impose on these filters, we again use the representation $\omega = (\omega_1, \omega_2, \omega_3)$.

Figure 2 shows a four-channel two-dimensional subband coding scheme where the analyzing filters are $\{\tilde{m}_0, \tilde{m}_1, \tilde{m}_2, \tilde{m}_3\}$ and the reconstruction is performed by $\{m_0, m_1, m_2, m_3\}$.

If the low-pass filters satisfy

$$m_0(0) = \tilde{m}_0(0) = 1, \tag{22}$$

then we can define, as in the one-dimensional case, the dual scaling functions and wavelets by (20) and (21). If this subband coding scheme has the property of perfect reconstruction for any signal, then the same arguments as in [CDF] show that under some conditions on the convergence of the infinite products in (20), and provided that the high-pass filters vanish at the origin, the families $\{(\psi_\varepsilon)_\gamma^j\}_{j\in\mathbf{Z},\gamma\in\Gamma,\varepsilon=1,2,3}$ and $\{(\tilde{\psi}_\varepsilon)_\gamma^j\}_{j\in\mathbf{Z},\gamma\in\Gamma,\varepsilon=1,2,3}$ are biorthogonal bases of $L^2(\mathbf{R}^2)$.

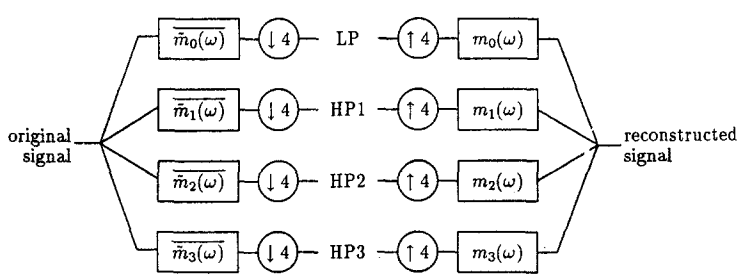

Fig. 2. A four-channel subband coding scheme: $4\downarrow$ stands for decimation, $4\uparrow$ for up-sampling (the reconstructed signal has to be normalized by a factor of 4).

These arguments are recalled in the Appendix. We now describe the properties of exact reconstruction.

2.2. Related Linear System

Define $\pi_0 = (0, 0, 0)$, $\pi_1 = (0, \pi, \pi)$, $\pi_2 = (\pi, 0, \pi)$, and $\pi_3 = (\pi, \pi, 0)$. The following two results characterize families of filters with exact reconstruction:

Lemma 2.2.1. *The family $m_0, \ldots, m_3$, $\tilde{m}_0, \ldots, \tilde{m}_3$ (hexagonal or not) has exact reconstruction if and only if it satisfies*

$$\begin{cases} \sum_{i=0}^{3} \overline{\tilde{m}_i(\omega)} m_i(\omega) = 1, \\ \sum_{i=0}^{3} \overline{\tilde{m}_i(\omega + \pi_1)} m_i(\omega) = 0, \\ \sum_{i=0}^{3} \overline{\tilde{m}_i(\omega + \pi_2)} m_i(\omega) = 0, \\ \sum_{i=0}^{3} \overline{\tilde{m}_i(\omega + \pi_3)} m_i(\omega) = 0. \end{cases} \tag{23}$$

Proof. The proof is exactly the same as the one-dimensional case (see [CDF]): it suffices to remark that the action of the subband coding scheme of Fig. 2 on a two-dimensional discrete signal $\{s_\gamma\}_{\gamma \in \Gamma}$ can be expressed on the discrete Fourier transform $s(\omega)$ by the formula

$$Rs(\omega) = \sum_{j=0}^{3} s(\omega + \pi_j) \sum_{i=0}^{3} \overline{\tilde{m}_i(\omega + \pi_j)} m_i(\omega), \tag{24}$$

where $Rs(\omega)$ is the discrete Fourier transform of the reconstructed signal. Perfect reconstruction for any discrete signal is thus equivalent to (23). ■

Lemma 2.2.2. *If the family $m_0, \ldots, m_3$, $\tilde{m}_0, \ldots, \tilde{m}_3$ of hexagonal compactly supported filters has exact reconstruction, then it satisfies*

$$m_0 = \frac{1}{D} \begin{vmatrix} \overline{\tilde{m}_1(\omega + \pi_1)} & \overline{\tilde{m}_2(\omega + \pi_1)} & \overline{\tilde{m}_3(\omega + \pi_1)} \\ \overline{\tilde{m}_1(\omega + \pi_2)} & \overline{\tilde{m}_2(\omega + \pi_2)} & \overline{\tilde{m}_3(\omega + \pi_2)} \\ \overline{\tilde{m}_1(\omega + \pi_3)} & \overline{\tilde{m}_2(\omega + \pi_3)} & \overline{\tilde{m}_3(\omega + \pi_3)} \end{vmatrix}, \tag{25}$$

where D is a nonzero constant and

$$\tilde{m}_0 \overline{m_0}(\omega) + \tilde{m}_0 \overline{m_0}(\omega + \pi_1) + \tilde{m}_0 \overline{m_0}(\omega + \pi_2) + \tilde{m}_0 \overline{m_0}(\omega + \pi_3) = 1. \tag{26}$$

Proof. Consider (23) as a system of equations in the unknown $\{m_0, \ldots, m_3\}$ with coefficients depending on $\{\overline{\tilde{m}_0}, \ldots, \overline{\tilde{m}_3}\}$. Since (23) has a nonzero solution in $\mathscr{C}\mathscr{F}$, its determinant has an inverse in $\mathscr{C}\mathscr{F}$, and therefore must be of the form $\mathrm{Det}(\omega) = De^{i(n_1\omega_1 + n_2\omega_2 + n_3\omega_3)}$.

Consequently, m_0 is given by

$$m_0(\omega) = \frac{M_0(\omega)}{\mathrm{Det}(\omega)} = e^{-i(n_1\omega_1 + n_2\omega_2 + n_3\omega_3)} \frac{M_0(\omega)}{D}, \tag{27}$$

where $M_0(\omega)$ is the minor of system (23) associated with $\tilde{m}_0(\omega)$ in the first line. However, by (19), M_0 obviously has invariance by $2\pi/3$, and m_0 must have this invariance too by the definition of an hexagonal family of filters. So that we must have

$$n_1 = n_2 = n_3, \tag{28}$$

which proves (25) (because $\mathrm{Det}(\omega) = D$).

If we now develop the determinant of system (23), using the symmetries expressed in (19), we obtain

$$\sum_{j=0}^{3} \bar{\tilde{m}}_0 M_0(\omega + \pi_j) = D, \tag{29}$$

from which we deduce (26). ■

For a given m_0, an $\tilde{m}_0$ satisfying (26) is called a dual to m_0. As in the one-dimensional case, this dual filter is not unique. It is easily checked that a filter b is a dual to a filter a if and only if ab becomes 1 (the unit in $\mathscr{C}\mathscr{F}$) after decimation. So that, for instance, if $a, b, c \in \mathscr{C}\mathscr{F}$, then ac is a dual to b if and only if a is a dual to bc. This elementary property is used later.

Remark 2.2.3. "Duality relation" (26) can be viewed as a simple generalization of relation (9) obtained in the one-dimensional case. For the high-pass filters, we can see from (25) that no more do we have a simple relation as in (10): it seems that we first need to know the high-pass filters to derive the low-pass filters. Instead of (26), the mapping (18) could be attempted to be used to generalize (10). Unfortunately this is not enough to satisfy system (23) except in the orthonormal case (when $m_i(\omega) = \tilde{m}_i(\omega)$ for $i = 0 \cdots 3$).

Remark 2.2.4. When $m_0(\omega)$ has hexagonal symmetry, given a dual filter $\tilde{m}(\omega)$, we can immediately derive a dual filter with hexagonal symmetry by the choice

$$\tilde{m}_0(\omega) = \tfrac{1}{3}(\tilde{m}(\omega) + \tilde{m}(\omega_2, \omega_3, \omega_1) + \tilde{m}(\omega_3, \omega_1, \omega_2)) \tag{30}$$

that still satisfies (26).

The results that we have proved in this section provide us with a systematic resolution scheme for (23).

2.3. Resolution

Here is an indication about how to solve (23):

Theorem 2.3.1. *Let $\tilde{m}_1$ be a compactly supported filter. Derive $\tilde{m}_2$ and $\tilde{m}_3$ by* (19) *and m_0 by* (25) *with an arbitrary $D \neq 0$. Let $\tilde{m}_0$ be a compactly supported*

dual to m_0 (that is, $\tilde{m}_0$ should satisfy (26)) *with hexagonal symmetry. Derive m_1 by the usual formula for a solution of* (23) *and m_2 and m_3 by* (19). *Then the family $\{m_0, \ldots, m_3, \tilde{m}_0, \ldots, \tilde{m}_3\}$ is hexagonal with exact reconstruction.*

Proof. $\{m_0, \ldots, m_3, \tilde{m}_0, \ldots, \tilde{m}_3\}$ is clearly hexagonal. Identities (25) and (26) imply that the determinant of the system is equal to D. We thus can derive m_1 as the second component of the solution of (23). The symmetries of this system imply that the last two components m_2 and m_3 can indeed be derived from m_1 by (19). This shows that system (23) is satisfied by this choice of filters. ■

Remark 2.3.2. We have mentioned that, to generate biorthogonal wavelet bases, m_0 and $\tilde{m}_0$ should be equal to 1 at the origin. This requirement fixes the value of D. The general procedure to design a subband coding scheme with exact reconstruction that may lead to wavelets is thus the following:

1. Choose the analysis high-pass filters with hexagonal symmetry.
2. Derive the synthesis low-pass filter by (25), imposing $m_0(0) = 1$.
3. Find an analysis low-pass filter that satisfies (26) and $\tilde{m}_0(0) = 1$.
4. Derive the synthesis high-pass filters by solving system (23).

Remark 2.3.3. It can be easily checked that if we exchange the families $\{m_0, \ldots, m_3\}$ and $\{\tilde{m}_0, \ldots, \tilde{m}_3\}$, system (23) is still satisfied (replace ω by $\omega + \pi_j$ in the jth line of the system and use $\hat{\Gamma}$-periodicity): perfect reconstruction is preserved by interchanging the analysis and synthesis filters (if these filters generate biorthogonal wavelets, this also mean that we interchange the analysis and synthesis wavelet). In particular, this means that $\tilde{m}_0(\omega)$ can be derived from $m_1(\omega)$ by formula (25).

Remark 2.3.4. Three problems arise here:

- Does (26) always have a solution in $\tilde{m}_0$ for a given m_0? Recall that such a solution is not unique in general.
- Given a family of exact reconstruction, compactly supported filters, do the associated wavelets form a Riesz base of $L^2(\mathbf{R}^2)$, and, if so, what is their regularity?
- What is the set of possible m_0? That is, which are the m_0 associated by (25) to some $\tilde{m}_1$? Can we at least find a family of "good" m_0's and some $\tilde{m}_1$ giving rise to them?

The first two questions will be precisely answered. The third remains mainly opened; here are some elements to answer it.

2.4. Possible Choices for m_0

To find an $\tilde{m}_1$ giving rise to a given m_0, a nonlinear (third-degree homogeneous) system in many unknowns has to be solved.

An $\tilde{m}_1$ with a given support gives rise to an m_0 with a much larger support (two successive convolutions happen in each term in (25)) although with more symmetry;

so that when the support of m_0 grows, it quickly becomes unlikely that a solution to (25) will be found.

For m_0 with a small support, however, things are different.

Proposition 2.4.1. *Let m_0 be an hexagonal filter with coefficients of the following type:*

$$\begin{pmatrix} & b & & c & \\ c & & a & & b \\ & b & & c & \end{pmatrix}$$

(a being positioned at the origin of Γ). There exist an $\tilde{m}_1$ such that m_0 is given by formula (25).

Proof. It can be easily checked that if the coefficients of m_1 are (x, y, z) with the origin on the "x," then (25) leads to an hexagonal filter in which coefficients are given by

$$4y^2\begin{pmatrix} & z & & x & \\ x & & -y & & z \\ & z & & x & \end{pmatrix}$$

so that all m_0's of the above form are associated through (25) with an $\tilde{m}_1$. ■

3. Linear Spline Wavelets

3.1. Two Examples

The filter which gives rise to the Courant interpolating function by repeated convolutions of scaled versions of itself as in (11) is given by

Definition 3.1.1. $c(\omega) = \frac{1}{4}(1 + \cos(\omega_1) + \cos(\omega_2) + \cos(\omega_3))$ is the affine box spline generator with coefficients

$$\tfrac{1}{8}\begin{pmatrix} & 1 & & 1 & \\ 1 & & 2 & & 1 \\ & 1 & & 1 & \end{pmatrix}$$

(the origin of Γ being on the "2").

This low-pass filter can be generated from different high-pass filters as shown by

Proposition 3.1.2. *$\tilde{m}_1^a = \frac{1}{4}(1 - e^{i\omega_1})(1 - e^{-i\omega_3})$ and $\tilde{m}_1^b = \frac{1}{4}(1 - e^{-i\omega_1})^2$ give rise through (25) to $m_0 = c$.*

Proof. It is a consequence of Proposition 2.4.1 for $\tilde{m}_1^b$, and left to the reader for $\tilde{m}_1^a$ (it is only a computation and can be done directly). ■

Remark 3.1.3. The existence of some $\tilde{m}_1$ having the above property is known from Proposition 2.4.1 above, so that finding the coefficients of $\tilde{m}_1^a$ and $\tilde{m}_1^b$ is merely a question of solving an equation. There might actually be other filters giving rise through (25) to $m_0 = c$ (for instance, the images of $\tilde{m}_1^a$ and of $\tilde{m}_1^b$ under some symmetry of c).

Since $c(\omega)$ generates the Courant interpolating function, if we can now find a correct dual for c, we shall obtain a hexagonal wavelet base with one set of functions (say, the synthesis functions) piecewise linear.

We now answer the first question of the existence of a dual filter.

3.2. Existence of a Dual

The following result is a generalization of the one-dimensional result which ensures the existence of a dual filter for $m(\omega)$ if and only if the z transform $m(z)$ has no pair of zero $\{z, -z\}$ (recall that the z transform is simply the meromorphic function obtained by replacing $e^{i\omega}$ by z in the transfer function). However, the one-dimensional result is essentially a consequence of the Bezout theorem which does not hold for dimensions higher than 1 and we had to find a different proof, which is rooted in a well-known theorem of commutative algebra, Hilbert's Nullstellensatz.

To enounce and prove this result, we come back to the standard representation $\omega = (\omega_1, \omega_2)$.

Lemma 3.2.1. *Let $m(\omega) = m(\omega_1, \omega_2)$ be a two-dimensional filter. There exist a filter p such that*

$$mp(\omega) + mp(\omega + (\pi, 0)) + mp(\omega + (0, \pi)) + mp(\omega + (\pi, \pi)) = 1 \tag{31}$$

(which is equivalent to the duality relation (26)) if and only if there does not exist $(z_1, z_2) \in (\mathbf{C}^*)^2$ such that (z_1, z_2), $(z_1, -z_2)$, $(-z_1, z_2)$, and $(-z_1, -z_2)$ are all zeros of the z-transform of the Fourier coefficients of m.

Proof. We can express (31) using the z transform as follows:

$$mp(z_1, z_2) + mp(-z_1, z_2) + mp(z_1, -z_2) + mp(-z_1, -z_2) = 1 \tag{32}$$

for all (z_1, z_2) in $(\mathbf{C}^*)^2$. Clearly, this implies that m cannot vanish on four points of the type (z_1, z_2), $(-z_1, z_2)$, $(z_1, -z_2)$, and $(-z_1, -z_2)$.

To prove the converse, we first transform $m(z_1, z_2)$ into a polynomial of $\mathbf{C}[z_1, z_2]$. Since $m(\omega_1, \omega_2)$ is a finite impulse response filter, there exist two integers ℓ_1 and ℓ_2 such that if we define

$$m^*(z_1, z_2) = z_1^{\ell_1} z_2^{\ell_2} m(z_1, z_2), \tag{33}$$

then $m^*(z_1, z_2)$ is in $\mathbf{C}[z_1, z_2]$. According to the hypotheses, the set of common

zeros of the polynomials $m^*(z_1, z_2)$, $m^*(-z_1, z_2)$, $m^*(z_1, -z_2)$, and $m^*(-z_1, -z_2)$ is included into the region $R = (C \times \{0\}) \cup (\{0\} \times C)$.

Hilbert's Nullstellensatz (see II, p. 164, of [ZS]) tells us that, for any polynomial $f(z_1, z_2)$ vanishing on R, there exists a positive integer n such that $f^n(z_1, z_2)$ is in the ideal generated by these four polynomials. In particular, if we take $f(z_1, z_2) = z_1 z_2$, this means that there exist four polynomials p_1^*, p_2^*, p_3^*, and p_4^* in $\mathbf{C}[z_1, z_2]$ and an integer $n \geq 0$ that we can impose to be even, such that

$$z_1^n z_2^n = m^* p_1^*(z_1, z_2) + m^* p_2^*(-z_1, z_2) + m^* p_3^*(z_1, -z_2) + m^* p_4^*(-z_1, -z_2).$$

If we now define $p^* = \frac{1}{4}(p_1^* + p_2^* + p_3^* + p_4^*)$, we clearly have

$$m^* p^*(z_1, z_2) + m^* p^*(-z_1, z_2) + m^* p^*(z_1, -z_2) + m^* p^*(-z_1, -z_2) = z_1^n z_2^n.$$

We conclude the proof of the lemma by choosing the filter p such that

$$p(z_1, z_2) = z_1^{\ell_1 - n} z_2^{\ell_2 - n} p^*(z_1, z_2). \qquad \blacksquare$$

Remark 3.2.2. This proof can be extended as it is to higher dimensions.

3.3. Effective Choice of the Dual $\tilde{m}_0$

We can use the lemma above to show that there exists a dual to $m_0 = c$. In fact, it can be seen directly that, since $\sum_{j=0}^{3} c(\omega + \pi_j) = 1$, a natural dual for c is given by the transfer function constantly equal to 1. However, this dual cannot be used since if would not lead to an L^2 scaling function $\tilde{\varphi}_0$ but to a Dirac measure centered in 0.

We therefore need to find a "better" dual.

Let $m_0' = m_0 c = c^2$; from the previous lemma we know that m_0' also has a dual $\tilde{m}_0'$; the minimal degree dual is easily computed to be given by the coefficients

$$\frac{1}{4}\begin{pmatrix} & -1 & & -1 & \\ -1 & & 10 & & -1 \\ & -1 & & -1 & \end{pmatrix}.$$

Since $\tilde{m}_0'$ is a dual to $m_0 c$, $\tilde{m}_0 = \tilde{m}_0' c$ is a dual to m_0. We have

(34)

$$\tilde{m}_0(\omega) = \tfrac{1}{8}(1 + \cos(\omega_1) + \cos(\omega_2) + \cos(\omega_3))(5 - \cos(\omega_1) - \cos(\omega_2) - \cos(\omega_3)).$$

In the Appendix it is checked that $\tilde{m}_0$ gives rise to an $L^2(\mathbf{R}^2)$ scaling function and to biorthogonal wavelet bases.

Summing up the results above, we have

Theorem 3.3.1. *There exists a biorthogonal hexagonal wavelet base of $L^2(\mathbf{R}^2)$ with ψ_1 piecewise affine, φ the "Courant interpolating function," and $\tilde{\varphi}$ and $\tilde{\psi}_1$ with compact support.*

Figures 3–6 show some graphs of the functions obtained.

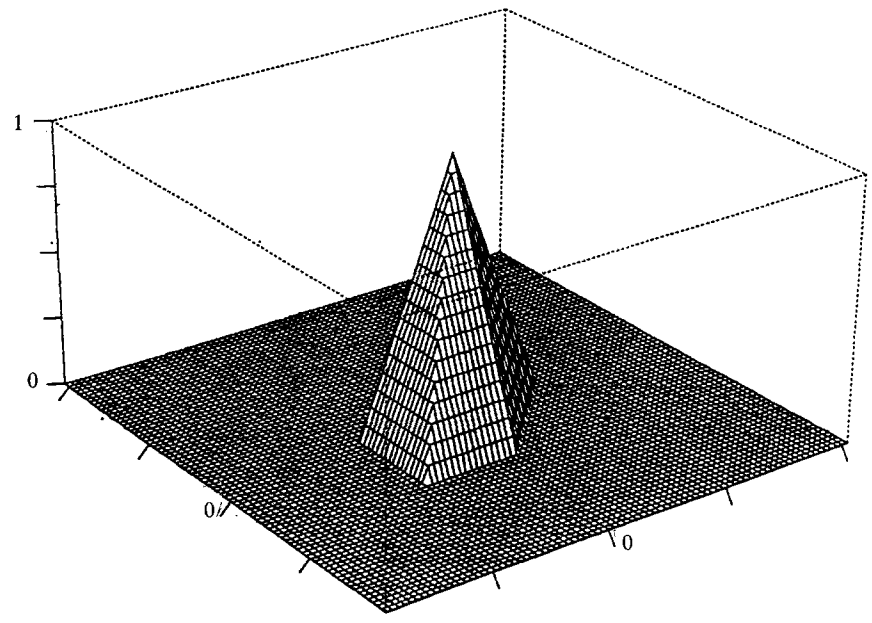

(a)

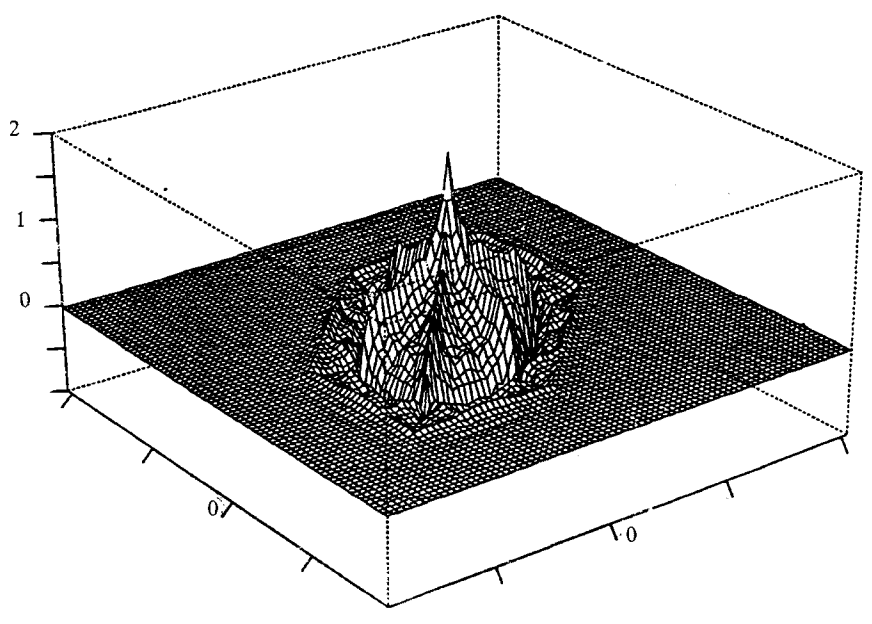

(b)

Fig. 3. Scaling functions associated with $c(\omega)$ and $\tilde{m}_0(\omega)$ given by (34). (a) The hat function $\varphi(x)$ and (b) the graph of $\tilde{\varphi}(x)$.

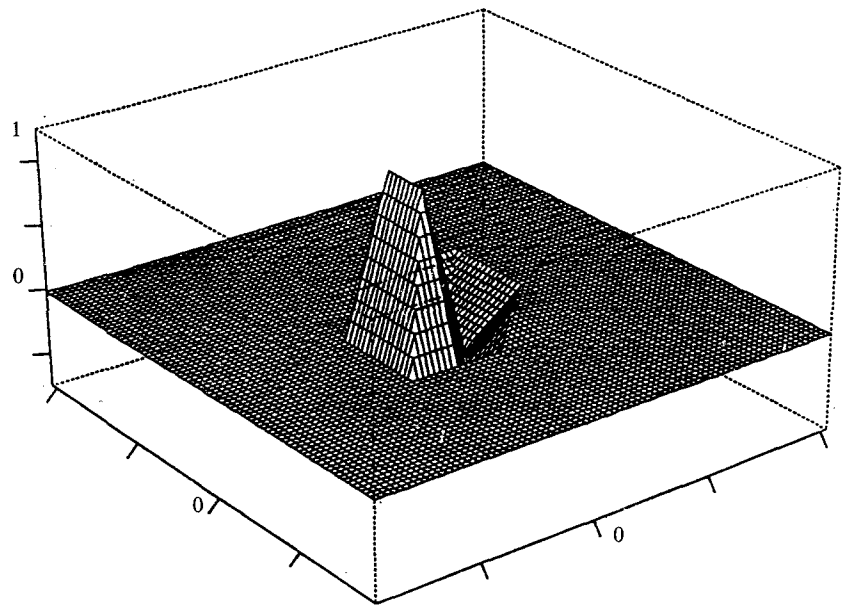

(a)

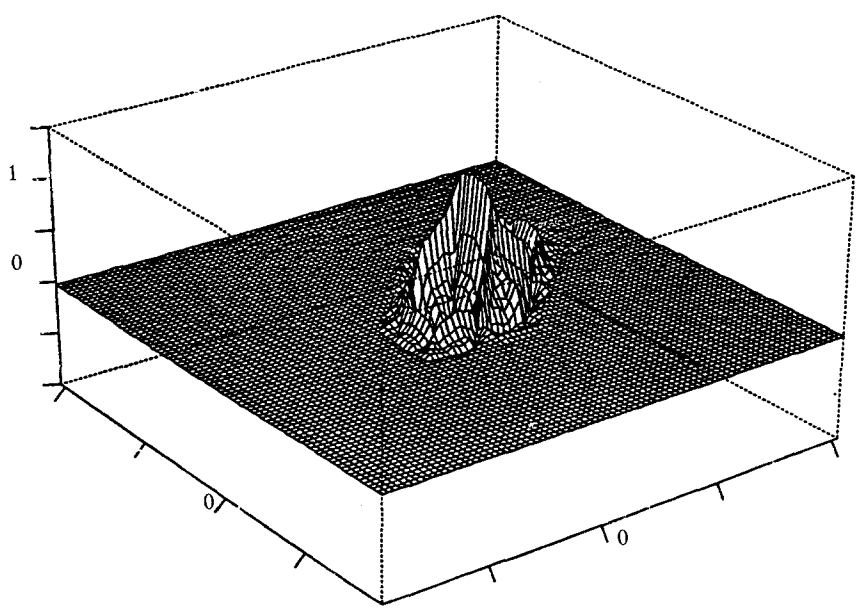

(b)

Fig. 4. Spline wavelet and dual wavelet associated with $m_1^a(\omega)$ and $\tilde{m}_1^a(\omega)$. The graphs of (a) $\psi_1^a(x)$ and (b) $\tilde{\psi}_1^a(x)$.

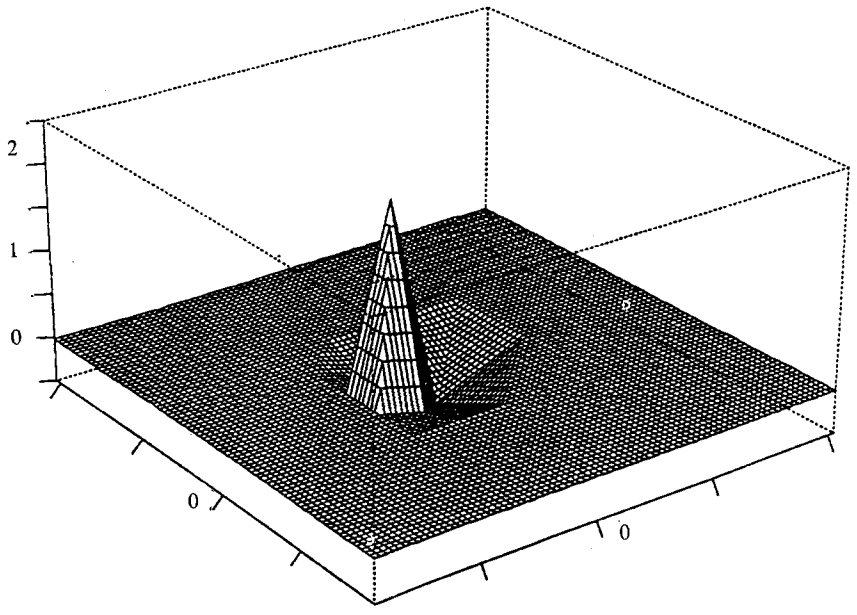

(a)

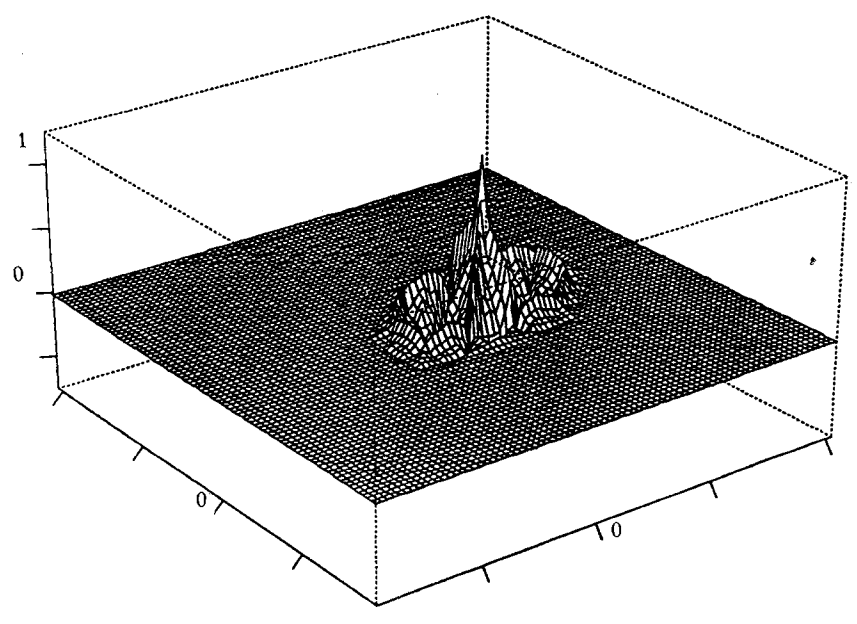

(b)

Fig. 5. Spline wavelet and dual wavelet associated with $m_1^b(\omega)$ and $\tilde{m}_1^b(\omega)$. The graphs of (a) $\psi_1^b(x)$ and (b) $\tilde{\psi}_1^b(x)$.

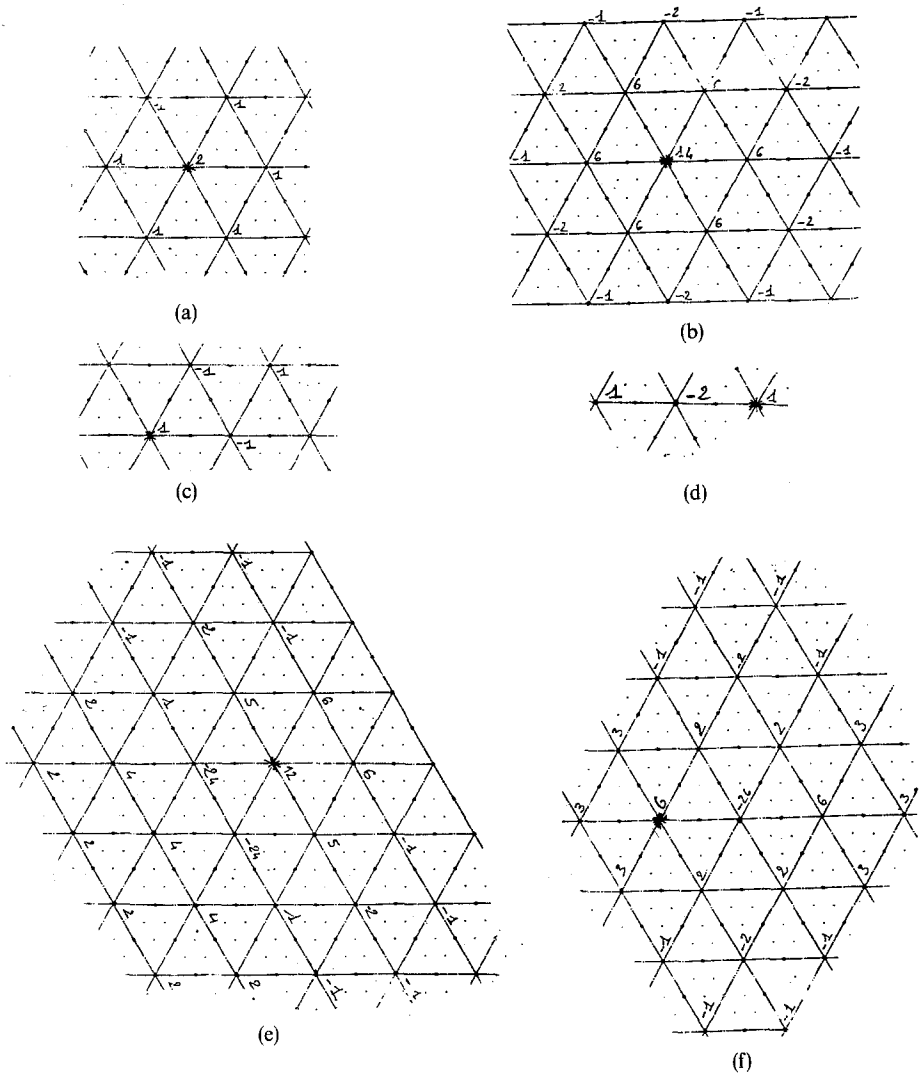

Fig. 6. Normalized filter coefficients in the spline case. The sign $*$ indicates the position of the origin. (a) $m_0(\omega)$ ($\times 8$), (b) $\tilde{m}_0(\omega)$ ($\times 32$), (c) $\tilde{m}_1^a(\omega)$ ($\times 4$), (d) $\tilde{m}_1^b(\omega)$ ($\times 4$), (e) $m_1^a(\omega)$ ($\times 16$), and (f) $m_1^b(\omega)$ ($\times 16$).

4. More Regularity

4.1. Motivations

It is necessary for some applications to have wavelet bases made of more regular functions. For instance, in image compression, it is necessary to use at least C^1 wavelets. Applications to mathematics typically require higher regularity.

Our goal here is to give hints and examples concerning hexagonal wavelets with some degree of smoothness.

This problem has been deeply studied in the unidimensional case [CD1], [D1], [D2]. In particular, it has been shown that multiplying the low-pass filter $m_0(\omega)$ by the factor $(1 + e^{i\omega})/2$ has the effect of increasing by one the Hölder and Sobolev exponent of the scaling function defined by (7). This "smoothing effect" can be explained simply: the function φ is convolved by the "box-function" $\chi_{[0,1]}$ generated by the filter $(1 + e^{i\omega})/2$. Using this fact, I. Daubechies has proved that arbitrarily high regularity could be attained in the orthonormal case by choosing an appropriate family of filters given by

$$m_0^N(\omega) = \left(\frac{(1 + e^{i\omega})}{2}\right)^N p_N(\omega). \tag{35}$$

The residual factor p_N (which is necessary to have (6)) has a negative effect on the regularity of φ but this effect is dominated by the positive action of the smoothing factor and this phenomenon increases with N.

In the hexagonal case we use the smoothing properties of $c(\omega)$ mainly in the same way as those of $(1 + e^{i\omega})/2$ in the one-dimensional case. We still have to show that it is possible to factorize $c(\omega)^N$ in our low-pass filters.

4.2. Theoretical Results

We prove the following result by using a "boot-strapping method":

Theorem 4.2.1. *For any p, q postive integers, there exists a family of exact reconstruction, compactly supported hexagonal wavelets* $m_0, \ldots, m_3, \tilde{m}_0, \ldots, \tilde{m}_3$ *such that* c^p *divides* m_0 *and* c^q *divides* $\tilde{m}_0$ *(in* $\mathscr{C}\mathscr{F}$*).*

Proof. We start by construction a first hexagonal family of filters $\{m'_0, \ldots, m'_3, \tilde{m}'_0, \ldots, \tilde{m}'_3\}$ by the following procedure:

1. Choose $\tilde{m}'_1 = \tilde{m}_1^a$ or $\tilde{m}_1^b$ (Definition 3.1.2).
2. Derive from Proposition 3.1.2 $m'_0 = c$.
3. Use Lemma 3.2.1 to find the smallest degree dual f to $c^q m'_0 = c^{q+1}$; then $\tilde{m}'_0 = c^q f$ is a dual to m'_0.
4. Find the m'_1 completing the family by solving the linear system (23) in $\mathscr{C}\mathscr{F}$.

We can then obtain the desired result in the following way:

5. Define $\tilde{m}_1 = m'_1$, so that, according to Remark 2.3.3, $m_0 = \tilde{m}'_0$.
6. Use Lemma 3.2.1 to find the smallest degree dual g to $c^p m_0 = c^{p+q} f$; then $\tilde{m}_0 = g c^p$ is a dual to m_0.
7. Find the m_1 completing the family by solving again the linear system (23) in $\mathscr{C}\mathscr{F}$.

The family of filters obtained obviously has all the desired properties. ■

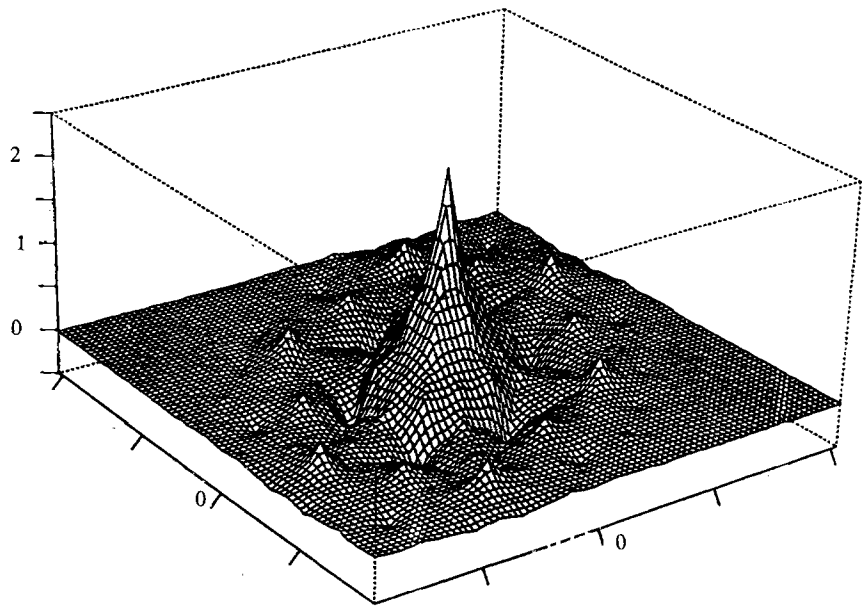

Fig. 7. The function $\tilde{\varphi}$ for $\tilde{m}_0 = \tilde{p}_0 c^2$ dual of $m_0 = c$.

4.3. Regularity

It is possible to compute explicitly the Sobolev regularity of the scaling function corresponding to a given filter; this comes from [CD1] and [CD2] and is briefly explained in the Appendix.

For small values of p and q, the regularity of the scaling functions does show an increase with p and q. However, since we do not have a simple expression for the residual factors f and g, we have no general result concerning the possibility of arbitrarily high regularity and in particular the asymptotic behavior of the Hölder exponent.

As an illustration, we give the graphs of $\tilde{\varphi}$ for $\tilde{m}_0 = \tilde{p}_0 c^2$ (Fig. 7) and $\tilde{\varphi}$ for $\tilde{m}_0 = \tilde{q}_0 c^3$ (Fig. 8), both dual to the Courant interpolating function φ, obtained by the method in the proof of Theorem 4.2.1.

4.4. How To Generalize this Procedure

The whole procedure, explained above, used to obtain exact reconstruction hexagonal families of compactly supported filters with c^p dividing m_0 and c^q dividing $\tilde{m}_0$ can be generalized by taking as m'_0 any filter such that cm'_0 has a dual; that is, any $\tilde{m}'_1$ giving rise through (25) to an m'_0 with this property can be used as a start for a "boot-strapping" method.

The only point is that, experimentally, most $\tilde{m}'_1$ are not so; for instance, we did not find directly any such $\tilde{m}'_1$ giving rise to an m'_0 that can be divided by c more than once; so that the c actually is a rather practical m'_0 to start with.

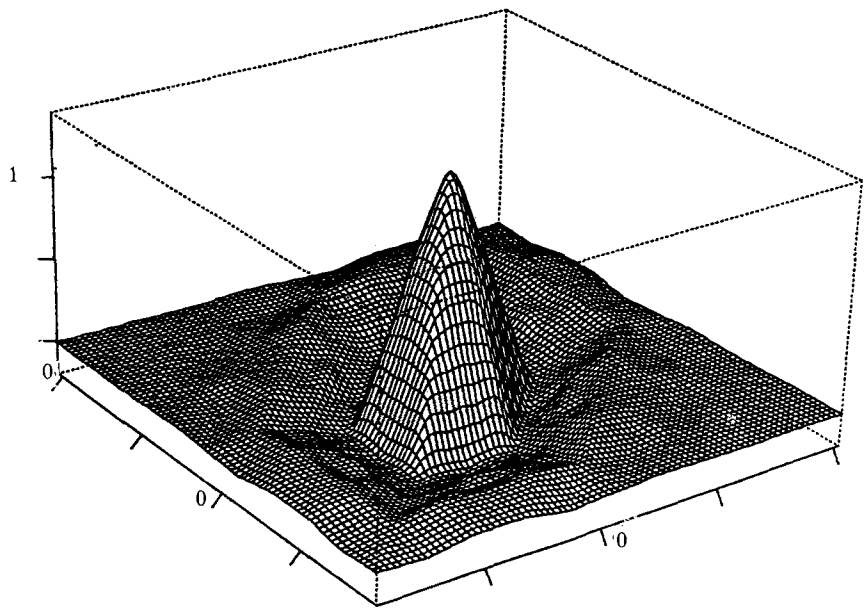

Fig. 8. The function $\tilde{\varphi}$ for $\tilde{m}_0 = \tilde{q}_0 c^3$ dual of $m_0 = c$.

Boot-strapping can also be repeated more than once; the families of filters obtained that way are different from those obtained through the proof of Theorem 4.2.1.

5. Angular Resolution in the Frequency Domain

5.1. Introduction

In this section we want to compare the tensor product decomposition and our hexagonal decomposition in terms of angular frequency resolution properties.

In some applications it is indeed interesting that each wavelet or, from a signal processing point of view, each high-pass channel in the subband coding scheme corresponds to a specific direction in the frequency plane. A typical example is the numerical analysis of "wave-fronts" which is an important issue in PDEs. It is necessary both to localize a singularity and to analyze its orientation or equivalently the directions in the frequency plane for which this singularity cases a bad decay at infinity. We already know that the wavelet analysis helps to characterize the singularities [Me]. We show here that wavelet-based techniques can be used to get informations about their orientation too.

5.2. With "Tensorial" Wavelets

In the tensor product decomposition if we assume that $m_0(\omega)$ is close to an ideal low-pass filter, i.e., the transfer function $\chi_{[-\pi/2,\pi/2]}(\omega)$, and that, similarly, $m_1(\omega)$ is

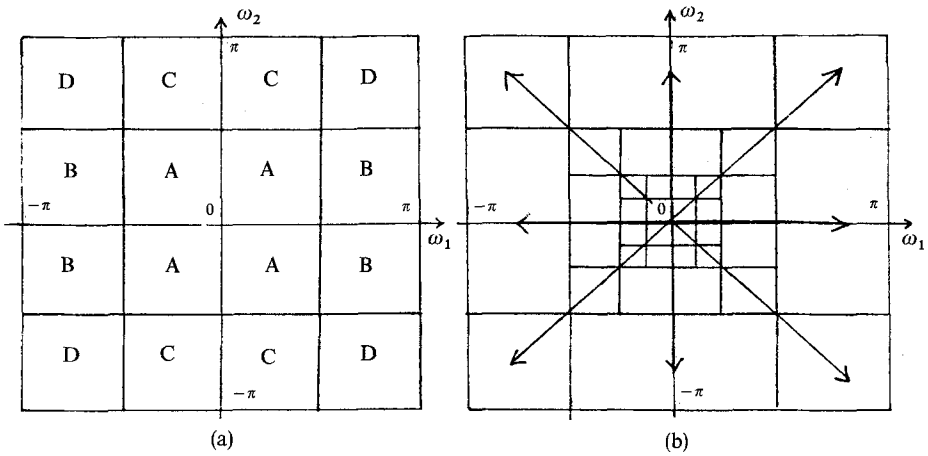

Fig. 9. The tensor product frequency decomposition: (a) one iteration and (b) three iterations.

close to an ideal high-pass filter, then the Nyquist domain $[-\pi, \pi]^2$ of a sampled signal is at the first step divided into nine regions corresponding to the four channels A, B, C, and D as shown in Fig. 9(a). The low-pass channel A is then decomposed again as we iterate the process (Fig. 9(b)). We see here that the high-pass channel corresponds to four directions in the frequency plane, horizontal for B, vertical for C, and diagonal for D. This cannot lead to a sharp angular resolution and, furthermore, there is an ambiguity since two directions contribute to the coefficients in channel D.

To increase the angular resolution, a possibility consists in iterating the decomposition not only on the low-pass channel A but also on the high-pass. This idea was developed in [CD3] and it is a particular case of the general construction of "wave-packets" introduced in [CMQW].

The result is shown in Fig. 10(a) in the case where we have made one decomposition on the high-pass channels. More directions have been obtained

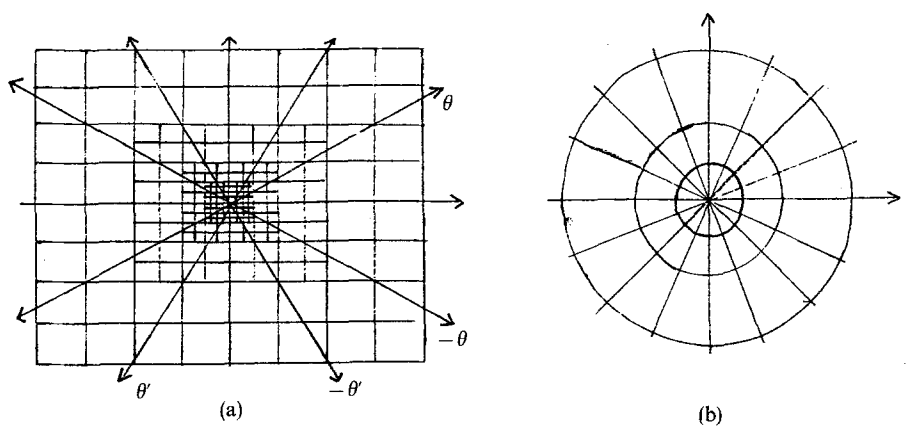

Fig. 10. (a) Wave packet type of frequency subdivision. (b) "Ideal situation" for angular resolution.

but the ambiguity has increased since we see that every channel corresponds to a couple of directions which is symmetrical with respect to the horizontal and vertical axes.

This ambiguity is a serious problem. Removing it by a second analysis where the data have been previously rotated by $\pi/4$ may be considered. That is, if we want to analyze a direction of angle θ, the first decomposition will include a channel corresponding to $(\theta, -\theta)$ and the second will include another channel corresponding to $(\theta, \pi/2 - \theta) = (\theta, \theta')$. Since $(\theta', -\theta')$ is also represented in the first decomposition and $(-\theta, \pi/2 + \theta) \sim (-\theta, \theta')$ in the second, we can write formally the following system which relates the energy of a signal in each direction and in each channel:

$$\begin{pmatrix} 1 & 1 & 0 & 0 \\ 0 & 0 & 1 & 1 \\ 1 & 0 & 1 & 0 \\ 0 & 1 & 0 & 1 \end{pmatrix} \begin{pmatrix} E(\theta) \\ E(\theta') \\ E(-\theta) \\ E(-\theta') \end{pmatrix} = \begin{pmatrix} E(\theta, \theta') \\ E(-\theta, -\theta') \\ E(\theta, -\theta) \\ E(\theta', -\theta') \end{pmatrix}. \tag{36}$$

Unfortunately we see here that the matrix is singular so this method fails.

More generally, it can be checked that it would fail for any rotation, the reason being that the rotation angle would have to be rational (otherwise directions would get really mixed up) and that the equivalent of the matrix in (36) would then still be a (bigger) matrix with only 0's and a fixed number of 1's in each line and each column, and that its determinant would again be 0.

All these remarks show the disadvantages of the tensor product construction for the angular frequency resolution. We are far from the ideal situation illustrated in Fig. 10(b) where every direction is uniformly distributed on dyadic rings. This situation could of course be attained by taking the Fourier transform of the signal and dividing the coefficients as in Fig. 10(b) but by doing this, all the spatial localization is lost.

5.3. With "Hexagonal" Wavelets

Let us now examine the new possibilities offered by our hexagonal construction.

In this case the Nyquist domain of a sampled signal is no longer $[-\pi, \pi]^2$ but is the hexagon X defined in the frequency plane by

$$X = \{|\omega_1 - \omega_2| \leq 2\pi\} \cap \{|\omega_2 - \omega_3| \leq 2\pi\} \cap \{|\omega_3 - \omega_1| \leq 2\pi\}. \tag{37}$$

As shown in Fig. 1(b), X is the Voronoi cell of the dual mesh $\hat{\Gamma}$ of Γ.

If we now assume that the high-pass filter $\tilde{m}_1(\omega)$, which is chosen at first in the process described in Section 1, is localized in the two half hexagons indicated as region 1 in Fig. 11(a), we find that the high-pass channels correspond to three directions and that there is no more ambiguity. The low-pass channel corresponds to the central hexagon.

If we iterate the decomposition in the high-pass regions similarly to the wave-packet decomposition of Fig. 10(a), we see (Fig. 11(b)) that no ambiguity is ever created. We can group the channels corresponding to the same direction as shown in Fig. 11(b). The result is now much closer to the ideal situation of Fig.

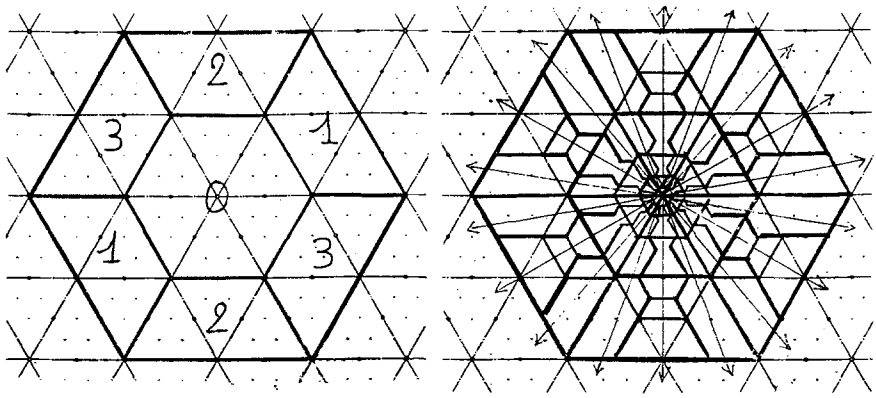

(a) (b)

Fig. 11. (a) The hexagonal frequency decomposition and (b) an example of the subdivision for a sharper angular resolution.

10(b) than with the tensor product construction. These new wavelets are thus quite appealing for their possibilities of angular resolution in the frequency plane.

Acknowledgments. This work was accomplished while Albert Cohen was at Bell Laboratories and J.-M. Schlenker was visiting there. We would like to thank the Mathematical Research Center for its hospitality and support. The authors are also grateful to the anonymous reviewers for many important remarks and suggestions in the revising process.

Appendix: Biorthogonality and Regularity Results in the Spline Case

A.1. Introduction

We prove in this appendix that in the case were the two dual low-pass filters are given by

$$m_0(\omega) = c(\omega) = \tfrac{1}{4}(1 + \cos\omega_1 + \cos\omega_2 + \cos\omega_3), \tag{A.1}$$

$$\tilde{m}_0(\omega) = \tfrac{1}{2}c(\omega)(5 - \cos\omega_1 - \cos\omega_2 - \cos\omega_3), \tag{A.2}$$

as in Section 3, then the associated functions ψ_ε and $\tilde{\psi}_\varepsilon$ ($\varepsilon = 1, 2, 3$) generate a pair of unconditional dual bases. That means that we have not only the biorthogonality relation

$$\langle \psi^j_{\varepsilon\gamma} | \tilde{\psi}^{j'}_{\varepsilon'\gamma'} \rangle = \delta_{j,j'}\delta_{\gamma,\gamma'}\delta_{\varepsilon,\varepsilon'} \tag{A.3}$$

for all $(j, j', \gamma, \gamma', \varepsilon, \varepsilon') \in \mathbf{Z}^2 \times \Gamma^2 \times \{1, 2, 3\}^2$, but also the frame bounds ensuring the stability of the decomposition and reconstruction algorithm, i.e., for all f in $L^2(\mathbf{R}^2)$,

$$A\|f\|^2 \le \sum_{j,\gamma,\varepsilon} |\langle f | \psi^j_{\varepsilon\gamma}\rangle|^2 \le B\|f\|^2, \tag{A.4}$$

$$\tilde{A}\|f\|^2 \le \sum_{j,\gamma,\varepsilon} |\langle f | \tilde{\psi}^j_{\varepsilon\gamma}\rangle|^2 \le \tilde{B}\|f\|^2. \tag{A.4'}$$

We also prove that the functions $\tilde{\varphi}$ and $\tilde{\psi}_\varepsilon$ are in a Sobolev space H^s, for some $s > 0$.

Note that if the functions φ and $\tilde{\varphi}$ are uniquely determined by the infinite products (26) and (35), there are several possibilities for ψ and $\tilde{\psi}$ which depend on the choice of $\tilde{m}_1(\omega)$ leading to $m_0(\omega) = c(\omega)$; but this choice does not play any role in the arguments that we use here, provided that the Fourier transform of the wavelets vanish at the origin.

A.2. Biorthogonality: General Case

In [CDF] a criterion for biorthogonality and frame bounds is introduced for wavelet bases of $L^2(\mathbf{R})$ and it can be reformulated for the hexagonal case in two dimensions.

For this, let us consider the hexagon defined in Section 1.4 by

$$X = \{|\omega_1 - \omega_2| \leq 2\pi\} \cap \{|\omega_2 - \omega_2| \leq 2\pi\} \cap \{|\omega_3 - \omega_1| \leq 2\pi\}. \tag{A.5}$$

X is the Voronoi cell of the dual mesh $\hat{\Gamma}$ of Γ (Fig. 11). It plays the same role as the interval $[-\pi, \pi]$ in one-dimensional theory. We define the functions φ_n and $\tilde{\varphi}_n$ by

$$\tilde{\varphi}_n(\omega) = \prod_{k=1}^{n} m_0(2^{-k}\omega)\chi_{2^n X}(\omega), \tag{A.6}$$

$$\hat{\tilde{\varphi}}_n(\omega) = \prod_{k=1}^{n} \tilde{m}_0(2^{-k}\omega)\chi_{2^n X}(\omega), \tag{A.6'}$$

where χ_A is the indicatrix function of a set A.

We now present the conditions for biorthogonality and stability:

Proposition A.2.1. *Equation* (A.3) *is ensured if* φ_n *and* $\tilde{\varphi}_n$ *tend to* φ *and* $\tilde{\varphi}$ *in* $L^2(\mathbf{R})$.

Proof. The proof is similar to the one-dimensional case presented in [CDF] and we just sketch it here:

- By using (23) and a recursion on n it is proved that

$$\langle \varphi_n(x - \gamma) | \tilde{\varphi}_n(x - \gamma') \rangle = \delta_{\gamma, \gamma'}, \qquad (\gamma, \gamma') \in \Gamma^2. \tag{A.7}$$

- Since we have the L^2 convergence, this leads to

$$\langle \varphi(x - \gamma) | \tilde{\varphi}(x - \gamma') \rangle = \delta_{\gamma, \gamma'}, \qquad (\gamma, \gamma') \in \Gamma^2. \tag{A.8}$$

- Equation (A.3) is a consequence of (A.8) and the relations (23) that relate the high-pass and low-pass filters. Indeed we can generalize (26) with, for all $(\varepsilon, \varepsilon') \in \{0, 1, 2, 3\}^2$,

$$\sum_{j=0}^{3} \overline{\tilde{m}_{\varepsilon'}} m_\varepsilon(\omega + \pi_j) = \delta_{\varepsilon, \varepsilon'}. \tag{A.9}$$

(For $\varepsilon = \varepsilon'$, (A.9) is the normalized determinant of (23) which is equal to 1. For $\varepsilon \neq \varepsilon'$, using the expression of m_ε as a minor of (23), (A.9) is a determinant which contains twice the same column and is thus equal to 0).

Equations (A.9) and (15) combined with (A.8) lead to the following relations for $(\varepsilon, \varepsilon', \gamma, \gamma') \in \{1, 2, 3\}^2 \times \Gamma^2$:

$$\langle \psi_\varepsilon(x-\gamma) | \tilde{\psi}_{\varepsilon'}(x-\gamma') \rangle = \delta_{\varepsilon,\varepsilon'} \delta_{\gamma,\gamma'}, \tag{A.10}$$

$$\langle \psi_\varepsilon(x-\gamma) | \tilde{\varphi}(x-\gamma') \rangle = \langle \varphi(x-\gamma) | \tilde{\psi}_\varepsilon(x-\gamma') \rangle = 0, \tag{A.11}$$

(A.3) is then obtained by scaling arguments similar to those in the proof of Lemma 3.7 in [CDF]. ■

Using the relation (A.9) we obtain, for any f in $L^2(\mathbf{R})$, the "telescoping formula"

$$\sum_{\gamma \in \Gamma} \langle f | \tilde{\varphi}_\gamma^{-J-1} \rangle \varphi_\gamma^{-J-1} = \sum_{j=-J}^{J} \sum_{\substack{\gamma \in \Gamma \\ \varepsilon = 1,2,3}} \langle f | \tilde{\psi}_{\varepsilon\gamma}^j \rangle \psi_{\varepsilon\gamma}^j + \sum_{\gamma \in \Gamma} \langle f | \tilde{\varphi}_\gamma^J \rangle \varphi_\gamma^J, \tag{A.12}$$

which expresses the refinement of a coarse approximation by adding details at each scale. When J tend to $+\infty$, the coarse approximation in the right member of (A.12) converges to zero in $L^2(\mathbf{R}^2)$ (this is easy to check as soon as φ and $\tilde{\varphi}$ are in $L^2(\mathbf{R}^2)$). The fine approximation in the left member tends to f in $L^2(\mathbf{R}^2)$ because of the following identity which is satisfied by any scaling function:

$$\sum_{\gamma \in \Gamma} \varphi(x-\gamma) = \sum_{\gamma \in \Gamma} \tilde{\varphi}(x-\gamma) = \int_{\mathbf{R}^2} \varphi = \int_{\mathbf{R}^2} \tilde{\varphi} = 1. \tag{A.13}$$

We thus have, for any f in $L^2(\mathbf{R}^2)$,

$$\lim_{J \to +\infty} \left\| f - \sum_{j=-J}^{J} \sum_{\substack{\gamma \in \Gamma \\ \varepsilon = 1,2,3}} \langle f | \tilde{\psi}_{\varepsilon\gamma}^j \rangle \psi_{\varepsilon\gamma}^j \right\|_{L^2(\mathbf{R}^2)} = 0. \tag{A.14}$$

Remark A.2.2. To prove the strong convergence of the series in (A.14) we need the frame bounds (A.4) and (A.4'). It is sufficient to check only the upper bounds since we then have

$$\begin{aligned} \|f\|^2 &= \lim_{J \to +\infty} \sum_{j=-J}^{J} \sum_{\substack{\gamma \in \Gamma \\ \varepsilon = 1,2,3}} \langle f | \tilde{\psi}_{\varepsilon\gamma}^j \rangle \langle \psi_{\varepsilon\gamma}^j | f \rangle \\ &\leq \left(\sum_{j,\gamma,\varepsilon} |\langle f | \tilde{\psi}_{\varepsilon\gamma}^j \rangle|^2 \right)^{1/2} \left(\sum_{j,\gamma,\varepsilon} |\langle f | \psi_{\varepsilon\gamma}^j \rangle|^2 \right)^{1/2} \end{aligned}$$

and the lower bounds follow.

Proposition A.2.3. *A sufficient condition for the upper bounds is given by*

$$|\tilde{\varphi}(\omega)| \leq C(1 + |\omega|)^{-1-\sigma}, \quad \sigma > 0, \quad \textit{for (A.4)}, \tag{A.15}$$

$$|\hat{\tilde{\varphi}}(\omega)| \leq \tilde{C}(1 + |\omega|)^{-1-\tilde{\sigma}}, \quad \tilde{\sigma} > 0, \quad \textit{for (A.4')}. \tag{A.15'}$$

Proof. The proof is the same as the first part of Lemma 3.4 in [CDF] (pp. 21–22). Note that (A.15) and (A.15') are not strictly necessary to have φ and $\tilde{\varphi}$ in $L^2(\mathbf{R}^2)$. ■

A.3. Biorthogonality: Application

We now have to check these conditions in the case where m_0 and $\tilde{m}_0$ are given by (A.1) and (A.2). This is easy in the case of the function φ. Indeed we have

$$\hat{\varphi}(\omega) = \frac{8}{\omega_1\omega_2\omega_3} \sin\left(\frac{\omega_1}{2}\right) \sin\left(\frac{\omega_2}{2}\right) \sin\left(\frac{\omega_3}{2}\right) \tag{A.16}$$

and

$$\hat{\varphi}_n(\omega) = \frac{8 \sin(\omega_1/2) \sin(\omega_2/2) \sin(\omega_3/3)}{2^{3n+3} \sin(\omega_1/2^{n+1}) \sin(\omega_2/2^{n+1}) \sin(\omega_3/2^{n+1})} \chi_{2^n X}(\omega). \tag{A.17}$$

It is clear that $\hat{\varphi}$ has enough decay for (A.15) and, moreover, φ_n satisfies

$$|\hat{\varphi}_n(\omega)| \leq C(1 + |\omega|)^{-2} \tag{A.18}$$

independently of $n \geq 1$. Thus φ_n tends to φ in L^2 by dominated convergence.

In the case of $\tilde{\varphi}$, proving the L^2 convergence of $\tilde{\varphi}_n$ appears to be more difficult. In fact $\hat{\tilde{\varphi}}(\omega)$ does not satisfy the decay condition (A.15′): indeed consider $v_0 = (2\pi/3, -2\pi/3, 0)$ and it successive dilations $v_n = (2^n\pi/3, -2^n\pi/3, 0)$. Clearly, we have

$$\begin{aligned} |\hat{\tilde{\varphi}}(v_n)| &= |\hat{\varphi}(v_0)|\, |\tilde{m}_0(v_0)|^n \\ &= |\hat{\varphi}(v_0)|(\tfrac{5}{8})^n \\ &= C|v_n|^{(\log 5 - \log 8)/\log 2} \end{aligned}$$

but $(\log 5 - \log 8)/\log 2 \geq -1$ and thus (A.15′) fails for $\tilde{\varphi}$. To derive the L^2 convergence of $\tilde{\varphi}_n$ to $\tilde{\varphi}$ and the upper frame bound in (A.4′) we use a sharper criterion which can be found in [CD1] and [CD2]. It is based on the study of the "transition operator" associated with the function $|\tilde{m}_0(\omega)|$. This operator acts on Γ^* periodic functions and it is defined by

$$\tilde{T}f(2\omega) = \sum_{j=0}^{3} |\tilde{m}_0|^2 f(\omega + \pi_j). \tag{A.19}$$

In [CD1], [CD2], and [C], the following properties were proved:

- If $\tilde{m}_0$ is a trigonometric polynomial, then the study of $\tilde{T}$ can be reduced to a finite-dimensional subspace $\tilde{E}$ generated by trigonometric polynomials. This is the case here.
- The subspace $\tilde{F} = \{f \in \tilde{E} | f(0) = 0\}$ is invariant by $\tilde{T}$ (this can be seen directly from (A-19)).
- For all 2π periodic function, we have (by recursion on n)

$$\int_X (\tilde{T})^n f(\omega)\, d\omega = \int_{\mathbf{R}^2} |\hat{\tilde{\varphi}}_n(\omega)|^2 f(2^{-n}\omega)\, d\omega. \tag{A.20}$$

The criterion obtained in [CD2] is the following:

Let $\tilde{\lambda}$ be the largest eigenvalue of $\tilde{T}$ restricted to $\tilde{F}$. If $|\tilde{\lambda}| < 1$, then $\tilde{\varphi}_n$ tend to $\tilde{\varphi}$ in L^2 and the upper frame bound in (A4′) is satisfied.

The proof of this result is based on a Littlewood–Paley estimation which can be made by taking a positive function $f(\omega)$ in $\tilde{F}$ and applying the Schwarz inequality on the first member in (A.20). This leads to

$$\int_{\mathbf{R}^2} |\hat{\tilde{\varphi}}_n(\omega)|^2 f(2^{-n}\omega)\, d\omega \leq C 2^{-\varepsilon n} \qquad \left(0 < \varepsilon < \frac{-\log|\lambda|}{\log 2}\right), \tag{A.21}$$

which ensures the L^2 convergence of $\tilde{\varphi}_n$ to $\tilde{\varphi}$ and if we set

$$\Delta_n = [-2^{n+1}\pi, -2^n\pi] \cup [2^n\pi, 2^{n+1}\pi],$$

we have

$$\int_{\Delta_n} |\hat{\tilde{\varphi}}(\omega)|^2\, d\omega \leq C 2^{-\varepsilon n} \qquad \left(0 < \varepsilon < \frac{-\log|\lambda|}{\log 2}\right). \tag{A.22}$$

Which is weaker than (A.15′) but is sufficient to ensure the upper frame bound in (A4′).

Moreover, we prove in [CD2] that this criterion is sharp, i.e., that the conditions $|\tilde{\lambda}| < 1$ and $|\lambda| < 1$ (for φ) are necessary and sufficient to construct biorthogonal bases. We thus only need to check the operator $\tilde{T}$ associated with $|\tilde{m}_0|^2$. Taking advantage of the symmetries, we consider the following trigonometric polynomials:

$$e_1 = 1,$$

$$e_2 = 2(\cos\omega_1 + \cos\omega_2 + \cos\omega_3),$$

$$e_3 = 2(\cos 2\omega_1 + \cos 2\omega_2 + \cos 2\omega_3),$$

$$e_4 = 2(\cos(\omega_1 - \omega_2) + \cos(\omega_2 - \omega_3) + \cos(\omega_3 - \omega_1)),$$

$$e_5 = 2(\cos 3\omega_1 + \cos 3\omega_2 + \cos 3\omega_3),$$

$$e_6 = 2(\cos(2\omega_1 - \omega_2) + \cos(2\omega_2 - \omega_1) + \cos(2\omega_2 - \omega_3) + \cos(2\omega_3 - \omega_2) + \cos(2\omega_3 - \omega_1) + \cos(2\omega_1 - \omega_3)).$$

Simple computations show that $\tilde{T}$ preserves the subspace $\tilde{E}$ generated by these six vectors and the matrix of $\tilde{T}$ has the following form:

$$m(\tilde{T}) = 2^{-8}\begin{pmatrix} 442 & 1128 & -228 & 0 & -24 & -384 \\ -38 & 120 & 379 & 320 & 124 & 376 \\ 1 & 4 & -26 & -64 & 196 & -64 \\ 6 & -56 & -74 & -8 & 0 & -320 \\ 0 & 0 & 1 & 0 & -4 & 8 \\ 0 & 0 & 7 & 4 & -28 & -32 \end{pmatrix}. \tag{A.23}$$

The spectrum contains 1 but it is a simple eigenvalue and is not included in the spectrum of $\tilde{T}$ restricted to the subspace $\tilde{F}$. The largest eigenvalue in $\tilde{F}$ is

$$\tilde{\lambda} = 0.54 < 1. \tag{A.24}$$

This allows us to conclude that the families

$$\{\psi_{\varepsilon\gamma}^j\}_{\gamma\in\Gamma, j\in\mathbf{Z}, \varepsilon=1,2,3} \quad \text{and} \quad \{\tilde{\psi}_{\varepsilon\gamma}^j\}_{\gamma\in\Gamma, j\in\mathbf{Z}, \varepsilon=1,2,3}$$

are biorthogonal Riesz bases of $L^2(\mathbf{R}^2)$.

Finally, by (A.22), we see that $\tilde{\varphi}$ and $\tilde{\psi}_\varepsilon$ are in the Sobolev space H^s for all

$$s < \frac{\log(\tilde{\lambda})}{2\log 2} \simeq 0.44.$$

References

[AS] E. Adelson, E. Simoncelli (1978): *Orthogonal pyramid transform for image coding.* Proceedings of the SPIE Conference on Visual Communication and Image Processing, pp. 50–58.

[BHR] C. de Boor, K. Höllig, S. Riemenschneider (1985): *Bivariate cardinal interpolation by splines on a three-dimension mesh.* Illinois J. Math., **29**:533–566.

[CSW] C. K. Chui, J. Stöckler, J. D. Ward (1990): Compactly Supported Box Spline Wavelets. CAT Report 230, Texas A&M University.

[C] A. Cohen (1991): *Biorthogonal wavelets.* In: Wavelet Analysis and Its Applications, (C. K. Chui, ed.). New York: Academic Press.

[CD1] A. Cohen, I. Daubechies (1991): *Nonseparable bidimensional wavelet bases.* Preprint, AT&T Bell Laboratories.

[CD2] A. Cohen, I. Daubechies (1991): *A stability criterion for biorthogonal wavelet bases and their related subband coding schemes.* Preprint, AT&T Bell Laboratories.

[CD3] A. Cohen, I. Daubechies (1992): *Orthonormal bases of compactly supported wavelets. Variation on a theme, II. Better frequency resolution.* SIAM J. Math. Anal.

[CDF] A. Cohen, I. Daubechies, J. C. Feauveau (1992): *Biorthogonal bases of compactly supported wavelets.* Comm. Pure Appl. Math., **41**.

[CMQW] R. R. Coifman, Y. Meyer, S. Quake, M. V. Wickerhauser (1990): *Signal processing and compression with wavelet packets.* Preprint, Department of Mathematics, Yale University.

[D1] I. Daubechies (1988): *Orthonormal bases of compactly supported wavelets.* Comm. Pure Appl. Math., **41**:909–996.

[D2] I. Daubechies (1991): Ten Lectures on Wavelets. Edited by SIAM.

[J] S. Jaffard (1989): Construction et propriétés des bases d'ondelettes. Remarques sur la controlabilité exacte. Ph.D. Thesis, Ecole Polytechnique.

[Ma] S. Mallat (1989): *A theory for multriesolution signal decomposition: the wavelet representation.* IEEE Trans. Pattern Anal. Mach. Intell., **2**(7).

[Me] Y. Meyer (1990): Ondelettes et operateurs. Paris: Hermann.

[ZS] O. Zarisky, P. Samuel (1958, 1960): Commutative Algebra, vols, I and II. Princeton, NJ: Van Nostrand.

A. Cohen
CEREMADE
Université Paris IX
75 016 Paris
France

J.-M. Schlenker
Centre de Mathématiques
Ecole Polytechnique
91 128 Palaiseau Cedex
France